CHARACTERIZATION AND OPTIMIZATION OF A RESONANT CAVITY ENHANCED P-i-N PHOTODIODE RESPONSE

Dušan S. Golubović, Petar S. Matavulj, and Jovan B. Radunović

Faculty of Electrical Engineering, University of Belgrade, P. O. Box 35-54
Bulevar revolucije 73, 11120 Belgrade, Yugoslavia

Abstract

This paper presents linear pulse response of a Resonant Cavity Enhanced (RCE) P-i-N fotodiode. The RCE P-i-N photodiode designed for high-speed aplication is analysed for various submicron thicknesses of absorption layer, bias voltages, active areas and incident pulse optical excitations. The results are obtained by numerical simulation of the complete phenomenological model for two valley semiconductor. Great enhancement of the quantum efficiency and the product bandwidth-quantum efficiency, is obvious from obtained results for this photodiode type.

Keywords: bandwidth, linear response, P-i-N photodiode, quantum efficiency, Resonant Cavity Enhanced photodiode.

1. Introduction

The photodetector bandwidth and sensitivity are the most critical factors in a new high bit rate optical communication sistems [1], [2]. Although a conventional P-i-N photodiodes are frequently used they are not the most convinient solution. The quantum efficiency of a conventional P-i-N photodiode is [1]

$$\eta = 1 - e^{-\alpha \cdot d} \quad , \tag{1}$$

α is an absorption coefficent and d is a thickness of i-layer. For the very wide list of relevant operating parameters, conventional P-i-N photodiode has the bandwidth maximum in submicron region of absorption layer thicknesses [1]. But, it is not applicable because the quantum efficiency in submicron region is very small. The quantum efficiency enhancing demands increasing of the absorption layer thickness. Increasing of the absorption layer thickness results in decreasing of a photodiodes bandwidth. Generaly speaking, it is not possible to provide simultaneously the maximal bandwidth and the maximal quantum efficiency.

A Resonant Cavity Enhanced (RCE) P-i-N photodiode is designed to provide simultaneously the large bandwidth and the large quantum efficiency [2]. Absorption layer with submicron thicknesses is put inside of a Fabry-Perot cavity. Owing

to interference effects electron-hole generation rate, which is proportional to the light intensity in the absorption layer, may be greatly enhanced. Therefore, with RCE P-i-N photodiode large quantum efficiency may be achieved with submicron thicknesses of absorption layer. Quantum efficiency of a RCE P-i-N photodiode is [3], [4], [2]

$$\eta = (1 - R_1)\frac{(1 - e^{-\alpha d})(1 + R_2 e^{-\alpha d}) + \frac{2\sqrt{R_2}\alpha}{\beta} e^{-\alpha d}\sin(\beta d)\cos(\beta d + \phi_2)}{1 - 2\sqrt{R_1 R_2} e^{-\alpha d}\cos(2\beta d + \phi_1 + \phi_2) + R_1 R_2 e^{-2\alpha d}} \quad . \tag{2}$$

R_1 and R_2 are the power reflectivies of the reflectors, ϕ_1 and ϕ_2 are corresponding phase shifts, λ is the wavelength of an incident optical radiation and β is the propagation constant. α and d have same meaning as in equation (1). The Fig. 1 shows quantum efficiency versus thickness of the absorption layer in case of conventional and RCE P-i-N photodiode in submicron region of the absorption layer thicknesses. Oscilatory behavior of the RCE P-i-N photodiodes quantum efficiency is result of

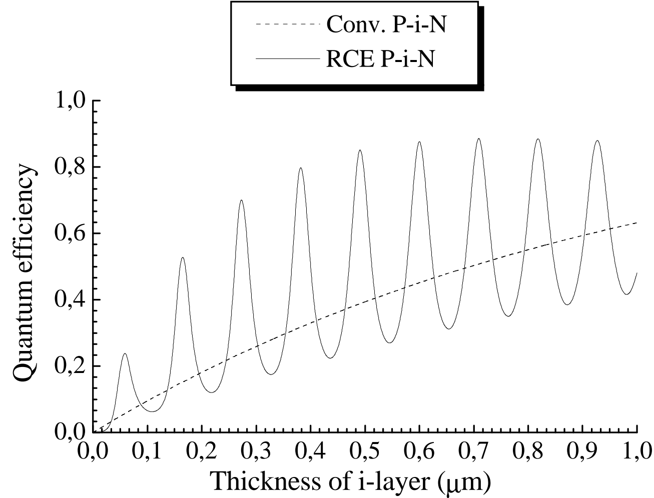

Fig. 1. Dependence of quantum efficiency on the thickness of apsorption layer for both conventional and RCE P-i-N photodiode. Reflectors parameters are $R_1 = 0.3$, $R_2 = 0.9$, $\phi_1 = 0$, $\phi_2 = \pi$, and the wavelength is $\lambda = 0.8\mu m$. The absorption coefficent and the refractive index correspond to GaAs.

resonant cavity presence. For the thicknesses of the absorption layer corresponding to the quantum efficiency maximums waves confinated between the reflectors constructively interfere, and for the thicknesses corresponding to the quantum efficiency minimums waves destructively interfere. It is noticeable that the quantum efficiency of the RCE P-i-N photodiode is, for certain i-layer thicknesses, more

than 100% larger than the quantum efficiency of the conventional P-i-N photodiode. If RCE P-i-N photodiode is fabricated with the submicron absorption layer thicknesses coresponding to the quantum efficiency maximums (Fig. 1.), it is possible to achieve the large bandwidth (because of the small submicron thicknesses of absorption layer) and the large quantum efficiency simultaneously.

2. The Model

A RCE P-i-N photodiode with absorption layer made of two valley semiconductor (GaAs) is considered. The photodiode general structure is shown in Fig. 2 [2]. The equivalent electric circuit of the RCE P-i-N photodiode is the same as

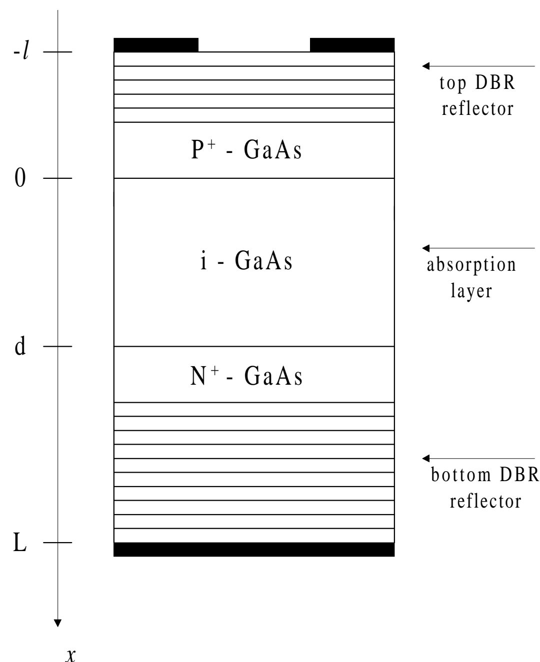

Fig. 2. General structure of the RCE P-i-N photodiode.

the equivalent electric circuit of the conventional P-i-N photodiode. Equivalent circuit used for detection is shown in Fig. 3 [1]. The detected signal is denoted as $V_R(t)$, $V(t)$ is the voltage on the reversed biased RCE P-i-N photodiode and $I(t)$ is the photocurrent. R is load resistance. Resistance of the diode contacts and the external parasitic capacitance are neglected [1], while the influence of the RCE P-i-N photodiode capacitance is taken into account by the displacement current.

During the detection of incident optical radiation, generated photocurrent causes a voltage drop on the load resistance. Therefore, the RCE P-i-N photodiode voltage is not constant during the detection. According to the Fig. 3 RCE P-i-N

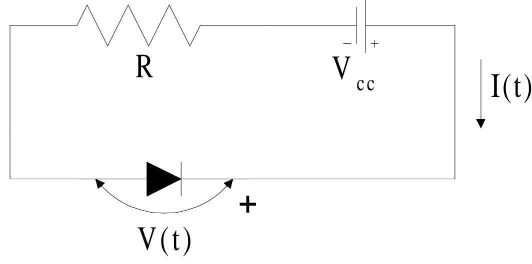

Fig. 3. Equivalent electric circuit of the RCE P-i-N photodiode used in detection.

photodiodes voltage is

$$V(t) = V_{cc} - R \cdot I(t) \quad . \tag{3}$$

The change of the voltage causes a perturbation of the electric filed in the structure, and therefore has influence on carrier transit time and the bandwidth of a photodiode [5].

Electric field has two components $K_W(x,t)$ and $K_{PH}(x,t)$. $K_W(x,t)$ is determined by the concentration of fixed charges in absorption layer and variable voltage on the RCE P-i-N photodiode.

$$K_W(x,t) = \begin{cases} -\frac{qN}{\varepsilon}(\mathrm{w}(t) - x), & 0 \le x \le \mathrm{w}(t) \quad (\mathrm{w}(t) \le d) \\ -\frac{qN}{\varepsilon}(d - x) - \frac{V(t) - V_D(d)}{d}, & 0 \le x \le d \quad (\mathrm{w}(t) > d) \\ 0, & \text{otherwise} \end{cases} \quad , \tag{4}$$

w(t) is the width of the depletion layer

$$\mathrm{w(t)} = \sqrt{\frac{2 \cdot \varepsilon \cdot \mathrm{V(t)}}{\mathrm{q \cdot N}}} \tag{5}$$

and $V_D(d)$ is punchthrough voltage

$$V_D(d) = \frac{q \cdot N \cdot d^2}{2 \cdot \varepsilon} \quad . \tag{6}$$

In equations (4) - (6) N denotes the small residual donor concentration in the absorption layer, ε is the dielectric constant of GaAs, d is the absorption layer thickness and $V(t)$ is RCE P-i-N photodiode voltage. $K_{PH}(x,t)$ is the electric field induced by the photogenerated carriers. $K_{PH}(x,t)$ is calculated with Poisson equation

$$\frac{\partial K_{PH}(x,t)}{\partial x} = \frac{q}{\varepsilon} \cdot (p(x,t) - n_1(x,t) - n_2(x,t)) \quad , \tag{7}$$

$p(x,t)$ is the concentration of the holes, $n_1(x,t)$ is concentration of electrons in the central valley and $n_2(x,t)$ is concentration of electrons in the satellite valley. Total electrical field in the RCE P-i-N photodiode in case of weak optical excitation is [1]

$$K(x,t) = K_W(x,t) + K_{PH}(x,t) \; (= K_W(x,t)) \quad . \tag{8}$$

Analysis of two valley semiconductor requires certain modifications of the continuity equations [1]. It is necessary to include electrons in satellite valleys and electron intravalley transfer. The continuity equations for electrons [2] and holes are

$$\frac{\partial n_1(x,t)}{\partial t} - \frac{1}{q} \cdot \frac{\partial j_1(x,t)}{\partial x} = G(x,t) + g(x,t) \quad , \tag{9}$$

$$\frac{\partial n_2(x,t)}{\partial t} - \frac{1}{q} \cdot \frac{\partial j_2(x,t)}{\partial x} = -g(x,t) \quad , \tag{10}$$

$$\frac{\partial p(x,t)}{\partial t} + \frac{1}{q} \cdot \frac{\partial j_p(x,t)}{\partial x} = G(x,t) \quad . \tag{11}$$

Equations (9) - (11) should be solved together with the drift-diffusion equations for the optically generated carriers. For electrons drift-diffusion equations are

$$j_i(x,t) = q n_i(x,t) v_i(x,t) + q \cdot \frac{\partial}{\partial x}(D_i n_i(x,t)) \quad i \in \{1,2\} \quad . \tag{12}$$

The total electron current is

$$j_n(x,t) = j_1(x,t) + j_2(x,t) \quad . \tag{13}$$

Drift-diffusion equation for holes is

$$j_p(x,t) = q p(x,t) v_p(x,t) - q \cdot \frac{\partial}{\partial x}(D_p p(x,t)) \quad . \tag{14}$$

Thus, the total conduction current in the RCE P-i-N photodiode is

$$j(x,t) = j_n(x,t) + j_p(x,t) \quad . \tag{15}$$

In equations (9) and (10) $g(x,t)$ denotes the net intravalley transfer rate which is given by [1]

$$g(x,t) = \frac{n_2(x,t)}{\tau_{21}(K(x,t))} - \frac{n_1(x,t)}{\tau_{12}(K(x,t))} \quad , \tag{16}$$

[1]This is the case which corresponds to linear photodiode response and the influence of photogenerated carriers (identical as influence of space charge) may be neglected. However, carrier transport cause exchanging place of carriers in absorption layer. It may be very important for calculation RCE P-i-N photodiode response, because of complex generation function. That's why we don't neglect second term in equation (8).

[2]Index 1 is adopted for electrons in central valley and index 2 for electrons in satellite valleys.

$\tau_{12}(K(x,t))$ and $\tau_{21}(K(x,t))$ are the phenomenological values of electron trasfer times from the central to the satellite valleys (τ_{12}) and vice versa (τ_{21}).

The pulsed optical generation rate $G(x,t)$ is

$$G(x,t) = \alpha I(x,t) \quad , \tag{17}$$

$$I(x,t) = (1-R_1)\frac{e^{-\alpha x} + 2\sqrt{R_2}e^{-\alpha d}\cos(2\beta(x-d)-\psi_2) + R_2 e^{-2\alpha d}e^{\alpha x}}{1-2\sqrt{R_1 R_2}e^{-\alpha d}\cos(2\beta d+\psi_1+\psi_2) + R_1 R_2 e^{-\alpha d}}\frac{W}{\frac{hc}{\lambda}A}\cdot\delta(t)$$

where $I(x,t)$ is the light intensity in the absorption layer. Fig. 4. depicts the optical generation in RCE P-i-N photodiode for two values of the absorption layer thicknesses in initial moment ($t=0$). When thickness of the absorption layer is

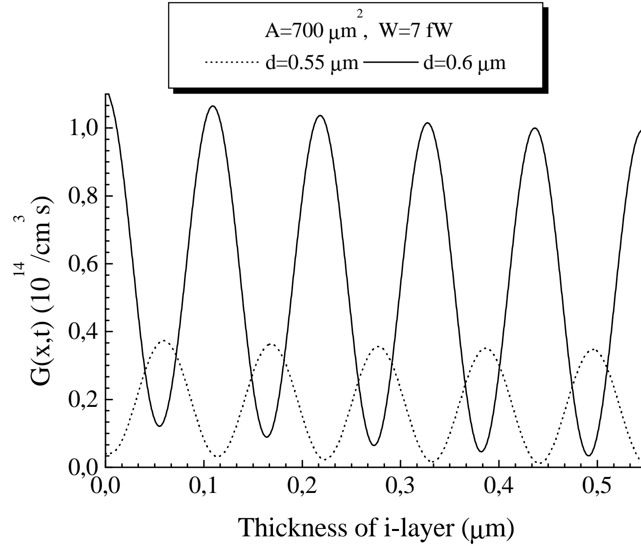

Fig. 4. Optical generation in GaAs RCE P-i-N fotodiode. Thicknesses of the absorption layer are $d = 0.55\,\mu m$ and $d = 0.6\,\mu m$, incident optical radiation power is $W = 7\,fW$, wavelength of the incident optical radiation is $\lambda = 0.8\,\mu m$, photodiodes active area is $A = 700\,\mu m^2$ and cavity parameters are $R_1 = 0.3$, $R_2 = 0.9$, $\phi_1 = 0$, $\phi_2 = \pi$.

$d = 0.6\,\mu m$, waves reflected in absorption layer, constructivly interfere and it is noticeable from Fig. 4. that the optical generation is signifficantly larger than in case of absorption layer thickness $d = 0.55\,\mu m$ when waves destructively interfere.

The dependence of the electron velocity on the electrical filed is

$$v_i(x,t) = \begin{cases} \mu_i \cdot K(x,t), & v_i < v_{is} \quad i \in \{1,2\} \\ v_{is}, & v_i \geq v_{is} \end{cases} \quad , \tag{18}$$

μ_1 and v_{1s} are the mobility and the saturation velocity of electrons in the central valley, respectively, and μ_2 and v_{2s} are the mobility and the saturation velocity of electrons in the satellite valleys. Similary, for the velocity of the holes is

$$v_p(x,t) = \begin{cases} \mu_p \cdot K(x,t), & v_p < v_{ps} \\ v_{ks}, & v_p \geq v_{ps} \end{cases} \quad , \tag{19}$$

μ_p is the mobility of the holes and v_{ps} is the saturation velocity of holes.

The RCE P-i-N photodiode response is given by [1], [5]

$$I(t) = \frac{A}{d}\int_0^d j(x,t)dx + \frac{\varepsilon A}{d}\frac{dV(t)}{dt} \quad . \tag{20}$$

The first term in equation (20) is conduction current ($j(x,t)$ is given by (15)) and the second term is the displacment current.

With the initial

$$\begin{array}{lcl} n_1(x,0) = p\,(x,0) & = & \alpha \cdot I(x,0) \\ n_2(x,t) & = & 0 \\ K(x,0) & = & K_W(x,0) \\ V(0) & = & V_{cc} \end{array} \tag{21}$$

and boundary conditions [1]

$$\begin{array}{lclcl} n_1(-l,t) & = & n_1(L,t) & = & 0 \\ n_2(-l,t) & = & n_2(L,t) & = & 0 \\ p\,(-l,t) & = & p\,(L,t) & = & 0 \end{array} \tag{22}$$

system of the equations described above is closed and provides to determine the current response.

In the above equations we neglect recombination, because we assume that considered processes are fast. Also, we neglect thermal generation because it creates the dark current that is neglible when compared to the photocurrent through range of investigation [1].

3. Numerical Tehhniques and Parameters of Calculation

The system described in previous section was solved by the method of finite differences, observing the stability condition [1]

$$v_{max}\Delta t \leq \Delta x \quad . \tag{23}$$

In equation (23) v_{max} is in fact v_{1s}, because the electron saturation velocity in central valley is the maximal velocity of the carriers. Adopted time step was $\Delta t = 10^{-4}\,s$ and the spatial step was chosen respecting condition (23). The bandwidth frequency is calculated using the fast Fourier transform applied to the current response.

The analysis of the response of the RCE P-i-N photodiode is performed using the parameters given in table I.

P^+	$=$	$10^{19}\,cm^{-3}$	N	$=$	$10^{14}\,cm^{-3}$	N^+	$=$	$10^{17}\,cm^{-3}$
l	$=$	$0.1\,\mu m$	d	$\leq$	$1\,\mu m$	L	$=$	$0.1\,\mu m$
α	$=$	$10^4\,cm^{-1}$	λ	$=$	$0.8\,\mu m$	ε_r	$=$	11.36
μ_1	$=$	$7500\,\frac{cm^2}{Vs}$	μ_2	$=$	$50\,\frac{cm^2}{Vs}$	μ_p	$=$	$150\,\frac{cm^2}{Vs}$
v_{1s}	$=$	$10^8\,\frac{cm}{s}$	v_{2s}	$=$	$10^7\,\frac{cm}{s}$	v_{ps}	$=$	$5\cdot 10^6\,\frac{cm}{s}$
D_1	$=$	$970\,\frac{cm^2}{s}$	D_2	$=$	$8.6\,\frac{cm^2}{s}$	D_p	$=$	$18.2\,\frac{cm^2}{s}$
R	$=$	$50\,\Omega$	W	$=$	$\left\{\begin{array}{l}0.07\\0.7\end{array}\right.\,fJ$	A	$=$	$\left\{\begin{array}{l}70\\700\end{array}\right.\,\mu m^2$
V_{cc}	$=$	$\left\{\begin{array}{l}0\\\vdots\\10\end{array}\right.\,\mathrm{V}$	R_1	$=$	0.3	R_2	$=$	0.9
ϕ_1	$=$	0	ϕ_2	$=$	π	n	$=$	3.67

Table 1. Parameters of the RCE P-i-N photodiode considered.

4. Results and Discussion

A linear response of the RCE P-i-N photodiode is considered in this paper. Applied power of the incident optical radiation ($W = 0.7\,fW$ for $A = 700\,\mu m^2$ and $W = 0.07\,fW$ for $A = 70\,\mu m^2$) provides photogenerated carrier concentration in initial moment ten times less than the concentration of donor impurities in absorption layer, which may be expressed as excitation level

$$\gamma = \frac{[n(x,0)]_{\max}}{N} = 0.1 \quad . \tag{24}$$

In case when $\gamma = 0.1$, influence of the space charge on the bandwidth may be neglected and therefore it is justified to analyse response as a linear [1].

Fig. 5. depicts linear current response of the RCE P-i-N photodiode for active areas $A = 700\,\mu m^2$ and $A = 70\,\mu m^2$ and reverse bias voltages $V_{cc} = 2\,V$ and $V_{cc} = 5\,V$. Thickness of the absorption layer is $d = 0.6\,\mu m$ and corresponds to the absolut quantum efficiency maximum. The cavity parameters are $R_1 = 0.3$, $\phi_1 = 0$ for the reflector on the illuminated side and $R_2 = 0.9$, $\phi_2 = \pi$ for reflector on the oposite side. These cavity parameters were constant during the simulations and therefore they will be not particularly emphasized in further considerations. Load resistance is $50\,\Omega$. From the Fig. 5. it may be seen that the response time is copletely independent on the applied bias voltage but it varies with change of the active area. In case of active area $A = 70\,\mu m^2$ the response time is about two times less then in case of active area $A = 700\,\mu m^2$. The response time determined with carrier transit time is independent on the photodiode active area but dependes on the applied bias voltage (transit time limited bandwidth [1]) and the response time determined with RC constant is independent on the applied bias voltage but dependes on the active area (RC limited bandwidth [1]). Therefore, we may

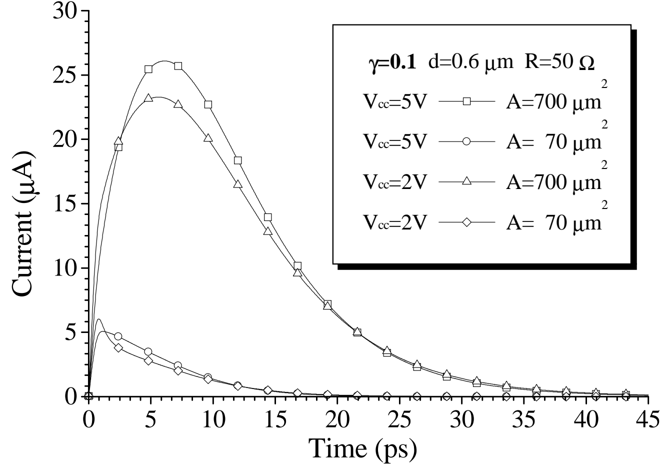

Fig. 5. Current response of the RCE P-i-N photodiode for active area $A = 70\,\mu m^2$ *and* $A = 700\,\mu m^2$*, reverse bias voltages* $V_{cc} = 2\,V$ *and* $V_{cc} = 5\,V$*, thickness of i-layer* $d = 0.6\,\mu m$*, excitation level* $\gamma = 0.1$ *and load resistance* $50\,\Omega$*.*

conclude that the response time is predominantly determined by parasitic RC constant. If we want to optimize speed of the photodiode we have to optimize the influenece of the RC constant on the response speed.

Fig. 6. shows dependence of the RCE P-i-N photodiode bandwidth on the thickness of the absorption layer in submicron region. Applied bias voltages are $V_{cc} = 0.2\,V$ and $V_{cc} = 0.5\,V$, photodiode active areas $A = 70\,\mu m^2$ and $A = 700\,\mu m^2$ and load resistance $50\,\Omega$. In the increasing region the bandwidth is limited with parasitic RC constant. The bandwidth determined with the RC constant is [1]

$$f_B = \frac{1}{2\pi RC} = \frac{d}{2\pi\varepsilon RA} \quad . \tag{25}$$

In equation (25) d is the absorption layer thickness, A is the photodiode active area and R is load resistance. As i-layer thickness incresases bandwidth also increases. In the decreasing region the bandwidth is predominantly determined with carrier transit time. When thicknees of the absorption layer increases carrier transit time increases and the bandwidth decreases. For the applied bias voltages electrons are loacalized in the central valley. Their speed is much larger than the speed of the holes and therefore holes are predominant limiting factor for the bandwidth. It is noticeable that all curves have maximum in submicron region, thus it is possible to choose the optimal absorption layer thickness which provides maximum speed of the RCE P-i-N photodiode. The maximal bandwidth and the optimal absorption layer thickness depend on the applied bias voltage and the photodiode active area.

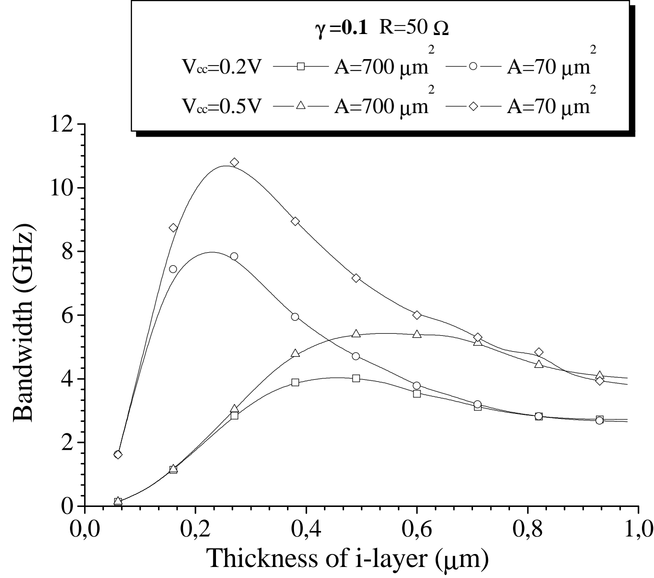

Fig. 6. The RCE P-i-N photodiode bandwidth versus thickness of absorption layer for the bias voltages $V_{cc} = 0.2\,V$ and $V_{cc} = 0.5\,V$ and active areas $A = 70\,\mu m^2$ and $A = 700\,\mu m^2$.

Fig. 7. depicts the RCE P-i-N photodiode bandwidth in the submicron region of the absorption layer thickness in case of the applied bias voltages $V_{cc} = 2\,V$ and $V_{cc} = 5\,V$, active areas $A = 70\,\mu m^2$ and $A = 700\,\mu m^2$ and load resistance $R = 50\,\Omega$. All curves have increasing part where the bandwidth is determined with parasitic RC constant. For the active area $A = 700\,\mu m^2$ bandwidth is determined by parasitic RC constant in entire submicron region. For the active area $A = 70\,\mu m^2$ the bandwidth curves have decreasing part in the submicron region of the absorption layer thicknesses. Large electric field values provide electrons localization in satellite valleys. In case of bias voltage $V_{cc} = 5\,V$ saturated holes are slower than non-saturated electrons for the absorption layer thicknesses $0.3\,\mu m \leq d \leq 0.6\,\mu m$ and they are predominant limiting factor. For the absorption layer thicknesses greater than $d = 0.6\,\mu m$ electrons in the satellite valleys are slower than holes and they become predominant limiting factor. For the reverse bias voltage $V_{cc} = 2\,V$ electrons are always slower than the holes and therefore they limit the bandwidth. Achieved maximum bandwidths of the RCE P-i-N photodiode are less than the bandwidths of the conventional P-i-N photodiode for the same operating parameters [3]. Reducement of the bandwidth is consequence of the displacement current influence. Owing to the interference effects in the absorption layer, carriers are generated in whole absorption layer (Fig. 4.). Therefore, time variation of the photogenerated

[3]The bandwidths of the conventional P-i-N photodiode are represented in [1].

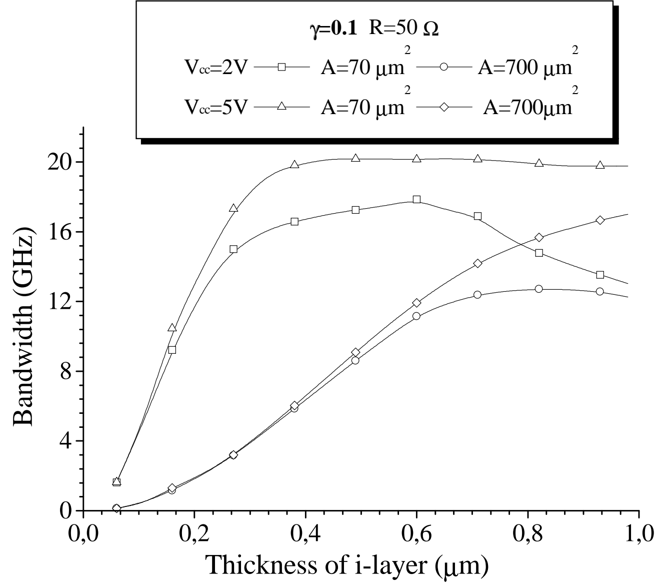

Fig. 7. The RCE P-i-N photodiode bandwidth versus thicknees of the absorption layer for the bias voltages $V_{cc} = 2\,V$ and $V_{cc} = 5\,V$ and active areas $A = 70\,\mu m^2$ and $A = 700\,\mu m^2$.

carrier concentrations in case of the RCE P-i-N photodiode is more complicated and more significant than in case of the conventional P-i-N photodiode. Carrier transport is more complex, too, and therefore displacement current has greater influence on total current than in case of the conventional P-i-N photodiode.

Fig. 8. depicts dependence of the RCE P-i-N photodiode bandwidth on the applied reverse bias voltage. Dash curve represents bandwidth limited only with carrier transit time ($R = 0\,\Omega$) and other two curves represent bandwidth when the parasitic RC constant is taken into account for the load resistance $R = 50\,\Omega$ and active areas $A = 700\,\mu m^2$ and $A = 70\,\mu m^2$. Thickness of the absorption layer is $d = 0.6\,\mu m$. We shall first consider the RCE P-i-N photodiode bandwidth limited only with carrier transit time. For the bias voltage $V_{cc} \leq 1\,V$ electrons are localized in central valley where their speed is much larger the the speed of the holes. Therefore, we may conclude that the bandwidth is limited by the hole component. When the applied bias voltage is $1\,V \leq V_{cc} \leq 2\,V$ electron intravalley transfer is present but the holes are still the main limiting factor. The electron intravalley transfer has (as it may be seen from Fig. 8[4]) influence on slope of the curve which represents the bandwidth versus the reverse bias voltage. For the bias voltages $V_{cc} > 2\,V$ electrons are predominantly localized in the satellite valleys. Owing to the electric field values they are not in the saturation, and they are slower

[4]This photodiode response is called nonstationary response [1].

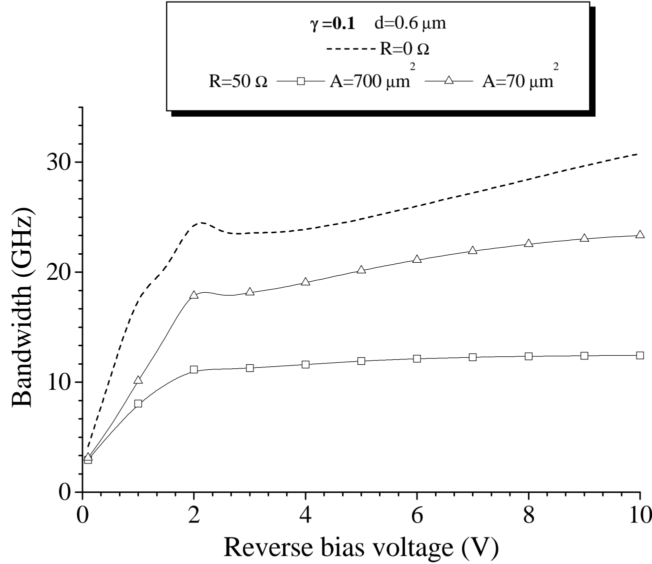

Fig. 8. The RCE P-i-N photodiode bandwidth versus the reverse bias voltage for the absorption layer thickness $d = 0.6\,\mu m$, load resistances $R = 0\,\Omega$ and $R = 50\,\Omega$ and active areas $A = 70\,\mu m^2$ and $A = 700\,\mu m^2$.

than the saturated holes. Thus, electrons predominantly limit the bandwidth. The slope of the bandwidth is significantly less owing to the small electron mobility in the satellite valleys. It is noticeable from Fig. 8. that presence of the RC constant reduces the bandwidth and decelerates the bandwidth slope. When the active area is $A = 70\,\mu m^2$ nonstationary effects, described above, are observed but their influence is less than in the case without the parasitic RC constant. When active area is $A = 700\,\mu m^2$ nonstationary effects have still less infulence and the curve slope is for $V_{cc} > 2\,V$ almost zero owing to the influence of the large time constant. For both values of the parasitic time constant, the bandwidth is limited with the carrier transit time.

The bandwidth-quantum efficiency product is used to present quality of achieved compromise between the speed and the sensitivity of the photodiode. Figs. 9a. and 9b. show the bandwidth-quantum efficiency product versus thickness of i-layer for both the conventional and the RCE P-i-N photodiode in case of active areas $A = 70\,\mu m^2$ and $A = 700\,\mu m^2$ and reverse bias voltages $V_{cc} = 2\,V$ and $V_{cc} = 5\,V$. In case of the conventional P-i-N photodiode, behaviour of the bandwidth-quantum efficiency product is predominantly determined by the bandwidth behaviour. Presence of the Fabry-Perot cavity, in case of the RCE P-i-N photodiode, has , as it may be seen from Figs. 9a. and 9b., significant influence on the behaviour of the bandwidth-quantum efficiency product. For the absorption layer thicknesses $d \leq 0.4\,\mu m$ the RCE P-i-N photodiode is less than in case

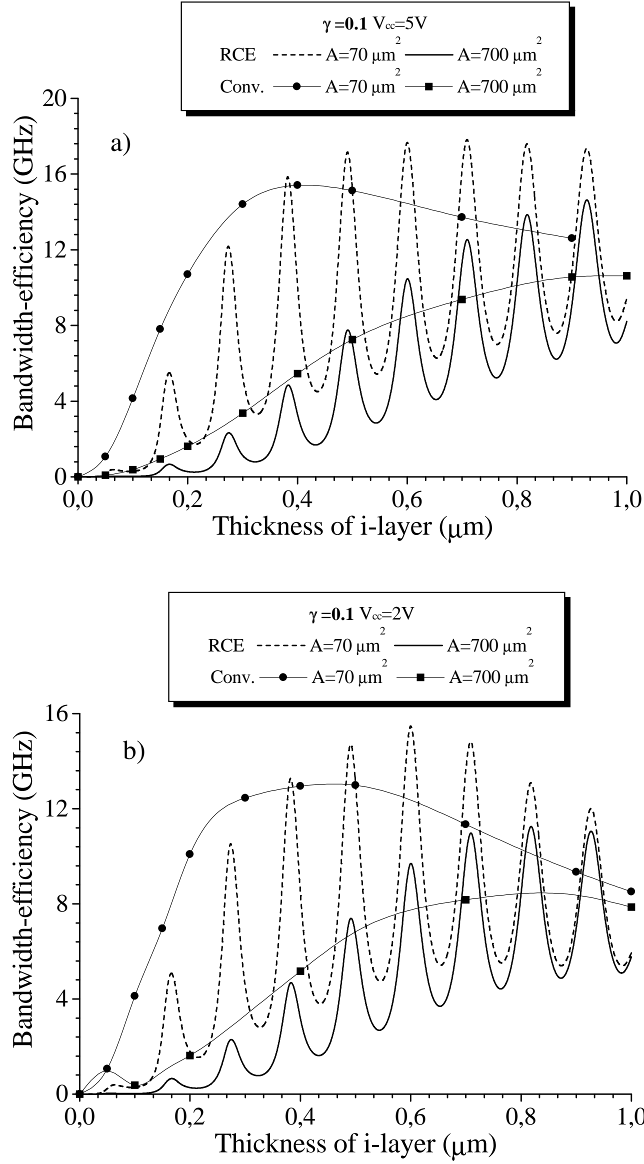

Fig. 9. The bandwidth-quantum efficiency product versus thickness of the absorption layer for both the conventional and the RCE P-i-N photodiode. Applied bias voltages are a) $V_{cc} = 5\,V$ and b) $V_{cc} = 2\,V$ (active areas $A = 700\,\mu m^2$ and $A = 70\,\mu m^2$).

of the conventional P-i-N photodiode. But, for certain thicknesses the bandwidth-quantum efficiency product is significantly larger than in case of the conventional P-i-N photodiode, for some thicknesses more than 40%. If RCE P-i-N photodiode is fabricated with those thicknesses of the absorption layer, the best rate between the speed and the sensitivity is achieved. Therefore, optimal thickness of the absorption layer, in sense of the best speed/sensitivity ratio, may be also defined. It is necessary to notice that the optimal absorption layer thickness which provides maximum bandwidth (maximum speed) and the optimal absorption layer thickness which provides the best speed/sensitivity ratio are two different thicknesses. Thus, when the RCE P-i-N photodiode operates with the best speed/sensitivity ratio, the photodiode speed, i. e. bandwidth does not correspond to the maximal achieved bandwidth. Values of the bandwidth-quantum efficiency product are determined with the cavity parameters and the photodiode operating parameters.

5. Conclusions

From the results presented above following conclusions may be derived.

- Presence of the resonant cavity greatly enhances quantum efficiency (maximum is about 90%, for $d = 0.6\,\mu m$, in considered case) for certain thicknesses of the absorption layer in submicron region. Therefore, the P-i-N photodiode may operate efficiently with the submicron thicknesses of absorption layer.

- The bandwidth has maximum in the submicron region of the absorption layer thicknesses. Thus, it is possible to chose the optimal absorption layer thickness which provides the maximum bandwidth, i. e. maximum speed of the RCE P-i-N photodiode. The maximum bandwidth and the optimal i-layer thickness depend on parasitic RC constant and applied reverse bias voltages.

- The bandwidth of the RCE P-i-N photodiode is less than the bandwidth of the conventional P-i-N photodiode for the same operating parameters owing to the significant influence of the displacement current, caused by complex carrier optical generation in the absorption layer. Therefore, the parasitic time constant has greater infuence on response of the RCE P-i-N photodiode than on response of the conventional P-i-N photodiode.

- The bandwidth-quantum efficiency product is significantly enhanced. For certain thicknesses of the i-layer, bandwidth-quantum efficiency product of the RCE P-i-N is about 40% larger than in case of the conventional P-i-N photodiode. For those thicknesses of the absorption layer the best ratio betwen the speed and the sensitivity is achieved.

References

[1] P. S. Matavulj, D. M. Gvozdić, and J. B. Radunović, "The Influence of Nonstationary Carrier Transport on the Bandwidth of P-i-N photodi-

ode", *Journal of Lightwave Technology*, vol. 15, no. 12, pp. 2270-2277, 1997.

[2] H. H. Tung and C. P. Lee, "Design of a Resonant-Cavity-Enhanced Photodetector for High-Speed Applications", *Journal of Quantum Electronics*, vol. 33,no. 5, pp. 753-760, 1997.

[3] P. L. Nikolić, D. M. Gvozdić, and J. B. Radunović, "Pulse Response of Resonant Cavity Enhanced Metal-Semiconductor-Metal Photodetector", *21st International Conference on Microelectronics (MIEL '97)*, vol. 1, pp. 327-330, 1997.

[4] M. S. Ünlü, Yusuf leblebici and Bora M. Onat, "Transient Simulation of Heterojunction Photodiodes - Part II: Analysis of Resonant Cavity Enhanced Photodetectors", *Journal of Lightwave Technology*, vol. 13, no. 3, pp. 406-415, 1995.

[5] P. S. Matavulj, D. M. Gvozdić, J. B. Radunović, and J. M. Elazar, "Nonlinear pulse response of P-i-N photodiode caused by the change of the bias voltage", *International Journal of Infrared and Millimeter Waves*, vol. 17, no. 9, 1996.